

UC San Diego

UC San Diego Previously Published Works

Title

Recommendations for interpreting zooplankton metabarcoding and integrating molecular methods with morphological analyses

Permalink

<https://escholarship.org/uc/item/4jm899dr>

Journal

ICES Journal of Marine Science, 78(9)

ISSN

1054-3139

Authors

Matthews, Stephanie A
Goetze, Erica
Ohman, Mark D

Publication Date

2021-11-25

DOI

10.1093/icesjms/fsab107

Peer reviewed



Recommendations for interpreting zooplankton metabarcoding and integrating molecular methods with morphological analyses

Stephanie A. Matthews ^{1,*}, Erica Goetze², and Mark D. Ohman ¹

¹California Current Ecosystem Long-Term Ecological Research Site, Integrative Oceanography Division, Scripps Institution of Oceanography, University of California San Diego, La Jolla, CA 92093, USA

²Department of Oceanography, School of Ocean and Earth Science and Technology, University of Hawai'i at Mānoa, Honolulu, HI 96822, USA

*Corresponding author: tel: (208) 304-8580; e-mail: samatthews@ucsd.edu

Matthews, S. A., Goetze, E., and Ohman, M. D. Recommendations for interpreting zooplankton metabarcoding and integrating molecular methods with morphological analyses. – ICES Journal of Marine Science, 0: 1–10.

Received 14 December 2020; revised 6 May 2021; accepted 18 May 2021.

Metabarcoding of zooplankton communities is becoming more common, but molecular results must be interpreted carefully and validated with morphology-based analyses, where possible. To evaluate our metabarcoding approach within the *California Current Ecosystem*, we tested whether physical subsampling and PCR replication affects observed community composition; whether community composition resolved by metabarcoding is comparable to morphological analyses by digital imaging; and whether pH neutralization of ethanol with ammonium hydroxide affects molecular diversity. We found that (1) PCR replication was important to accurately resolve alpha diversity and that physical subsampling can decrease sensitivity to rare taxa; (2) there were significant correlations between relative read abundance and proportions of carbon biomass for most taxonomic groups analyzed, but such relationships showed better agreement for the more dominant taxonomic groups; and (3) ammonium hydroxide in ethanol had no effect on molecular diversity. Together, these results indicate that with appropriate replication, paired metabarcoding and morphological analyses can characterize zooplankton community structure and biomass, and that metabarcoding methods are to some extent indicative of relative community composition when absolute measures of abundance or biomass are not available.

Keywords: *California Current Ecosystem*, community structure, metabarcoding, zooplankton, ZooScan

Introduction

The field of zooplankton ecology is beginning to embrace metabarcoding as an approach for describing spatial patterns in diversity and community composition, but there are some notable challenges in data interpretation. It remains difficult to link molecular estimates of diversity and community structure with morphological richness and abundance (Laakmann *et al.*, 2020), and the lack of standardization in metabarcoding methods makes it difficult to compare molecular richness across studies (Santoferrara, 2019). A better understanding of the relationship between metabarcoding and morphological analyses can help optimize methodological choices for studying zooplankton ecology (Bucklin *et al.*, 2019; Brisbin *et al.*, 2020). Here, we provide recommendations for best practices regarding subsampling, replication, and ethanol preserva-

tion. In addition, we test whether metabarcoding read counts are a suitable representation of relative biomass within the zooplankton community.

One of the strengths of metabarcoding is the ability to rapidly characterize community richness. Estimates of zooplankton richness using molecular markers can be up to an order of magnitude greater than morphological species richness (Laakmann *et al.*, 2020). The increased richness captured by metabarcoding may be due to detection of morphologically cryptic species, increased sensitivity to rare species, detection of intraspecific genetic variability (Brown *et al.*, 2015), or presence of pseudogenes or PCR chimeras. In contrast, many zooplankton metabarcoding pipelines require subsampling prior to DNA extraction which can potentially decrease observed richness (Loos and Nijland, 2020). Quantitative subsampling of bulk-fixed samples is a common procedure for

zooplankton analyses (Frolander, 1968; van Guelpen *et al.*, 1982), but the effects of subsampling on molecular diversity have not yet been tested.

A recurring challenge for metabarcoding is characterizing community structure from read counts (Laakmann *et al.*, 2020). While species richness is an important aspect of diversity, abundance and demographic structure are also important for understanding ecosystem dynamics (Elbrecht and Leese, 2015). PCR and sequencing biases can be normalized by including mock communities. This approach has been used for some studies of zooplankton communities (e.g. Hirai *et al.*, 2017) but remains relatively rare, and the effects of body composition, life history stage, cell count, copy number, and primer bias across diverse taxonomic groups are greater in metazoan than in microbial communities (Braukmann *et al.*, 2019). Despite these potential sources of bias, read counts have been positively correlated with morphologically identified abundance or biomass for some zooplankton taxa and in some ecosystems (Lindeque *et al.*, 2013; Hirai *et al.*, 2015; Harvey *et al.*, 2017; Bucklin *et al.*, 2019).

Preservation of field-collected zooplankton samples requires advance selection of a fixation protocol that is optimized for the target organisms and methods. The most common fixative for molecular analyses is 95–100% non-denatured ethanol (Loos and Nijland, 2020). However, ethanol is acidic and long-term storage of zooplankton tissue in ethanol can further increase acidity, resulting in dissolution of calcareous structures (Oakes *et al.*, 2019). This effect is particularly important for long-term preservation of calcifying organisms, when shell dissolution and changes in shell morphology may be interpreted as indicators of ocean acidification (e.g. Bednaršek *et al.*, 2017). Ammonium hydroxide has been used as a neutralizing agent for ethanol-preserved samples, successfully preserving pteropod shells for morphological analysis (Bednaršek and Ohman, 2015; Oakes *et al.*, 2019). However, the effect of ammonium hydroxide neutralization on molecular analyses is unknown.

In this study, we test the effects of subsampling, PCR replication, and preservation method on metabarcoding analysis of zooplankton community richness. We also directly compare paired metabarcoding and imaging analyses to test whether there is a relationship between read counts and morphology-based community composition at coarse taxonomic levels. We expected PCR replication to be a useful method for determining whether rare sequence variants are real or artifacts, and we expected minimal effects of physical subsampling on observed diversity. We also expected to find no relationship between normalized read counts and zooplankton abundance or biomass, given the many methodological steps at which biases could be introduced. We tested these questions using two molecular markers and ZooScan digital imaging of net-collected zooplankton samples from a range of environments across the California Current upwelling biome.

Methods

Zooplankton collection

Samples were collected between 29 April–8 May 2016 on cruise P1604 of the *California Current Ecosystem* LTER program using a depth-stratified 1 m² mouth area, 202 μ m mesh MOCNESS with paired day and night tows (Table S1). Sampling locations (designated “Cycles”; see Ohman *et al.*, 2013) ranged from the high-biomass nearshore upwelling environment to the offshore mesotrophic California Current. Zooplankton were sampled in 25

or 50 m vertical strata between the surface and 400 m. Each net-collected sample was quantitatively split with a Folsom splitter, then 50% fixed in 95% non-denatured ethanol neutralized with 5 mM ammonium hydroxide and 50% fixed in 1.7% formaldehyde buffered with sodium tetraborate. A total of 64 sets of paired ethanol and formaldehyde fixed samples were included in this analysis.

ZooScan Imaging

Zooplankton samples preserved in formaldehyde were imaged using a ZooScan (Gorsky *et al.*, 2010; Ohman *et al.*, 2012). Samples were size fractionated into 0.2–1.0-, 1.0–5.0-, and > 5-mm fractions. Quantitative subsamples of each were manually dispersed on the scanning surface, then digitally scanned. Images were segmented into regions of interest (ROIs) in ImageJ, and ROIs classified using machine-learning algorithms trained on manually sorted images of preserved zooplankton from the CCE (Ellen *et al.*, 2015). In addition, 100% of taxonomic assignments of ROIs were validated manually. Carbon biomass for each ROI was calculated from feret diameter using taxon-specific relationships between length and carbon (Lavaniegos and Ohman, 2007). Taxon abundance and carbon biomass were standardized for aliquot volumes and the volume of seawater filtered for each sample.

DNA extraction and amplification

Ethanol-fixed zooplankton samples were quantitatively split to a subsample small enough for DNA extraction with OMEGA EZNA Blood and Tissue Maxi kits (<5 g, typically 1/8–1/16th of the sample). Three to six subsamples were analyzed for four high biomass samples (subsequently termed “subsample replicates”; see Table S1). Subsample replicates were treated independently throughout extraction and amplification. DNA extractions were modified as previously described (Sommer *et al.*, 2017). Extraction negative controls were performed on a blank Nitex filter and included in all PCR steps. Eluent DNA concentrations were normalized to 20 ng μ l⁻¹ prior to PCR amplification.

To more broadly resolve the zooplankton community, two marker regions were amplified and sequenced. A 313-bp region of the mitochondrial cytochrome *c* oxidase subunit I gene (COI) was amplified with jgLCO1490 and jgHCO2198 (Leray *et al.*, 2013), and a 400-bp fragment in the V4 region of 18S was amplified using Uni18S and Uni18SR (Zhan *et al.*, 2013). Each subsample was amplified and sequenced in triplicate (subsequently termed “PCR replicates”). We used two-step PCR amplification and library preparation with duplicate dual indexing to mitigate index hopping, with unique indexes for PCR replicates to test for index biases and stochastic variability (Table S1 and S2; Costello *et al.*, 2018). The first reaction for each PCR replicate was duplicated, then the two reactions pooled and diluted as template for the indexing PCR (Table S2). All PCRs used high-fidelity “MyFi” polymerase (BioLine). Amplified DNA was bead-cleaned and final DNA concentrations quantified by Qubit or PicoGreen. Negative controls were included in sequencing runs if DNA was detected in the bead-cleaned product. Samples were pooled in equimolar concentrations and sequenced on two Illumina MiSeq runs (300bp paired-end V3).

Bioinformatic processing

Sequences were demultiplexed using cutadapt, and only sequences with exact matches to all four indexes retained (Martin, 2011).

Subsequent bioinformatic filtering in QIIME2 v. 2020.6.0 (Bolyen *et al.*, 2018) used marker-specific criteria as follows. For 18S, forward and reverse reads were truncated at 290bp and 275bp. Amplicon sequence variants (ASVs) were denoised independently for each sequencing run using DADA2 within QIIME2 with consensus chimera detection and pseudo-pooling (Callahan *et al.*, 2016). ASVs were not clustered in operational taxonomic units (OTUs) for 18S, as this gene region is highly conserved and even 99% OTUs can fail to resolve species-level differences (Clarke *et al.*, 2017). ASVs were aligned using MAFFT and taxonomy assigned using the 99% SILVA132 database, and by determining the lowest common ancestor (LCA) of up to five top *blastn* hits from GenBank (Pedregosa *et al.*, 2011; Yilmaz *et al.*, 2014; Clark *et al.*, 2016).

Sequences from COI were analyzed similarly. Forward and reverse reads were truncated at 280 and 250 bp. Denoised ASVs from DADA2 from each sequencing run were merged and clustered into *de novo* OTUs at 97% similarity using VSEARCH in QIIME2 (Rognes *et al.*, 2016). The 97% clustering threshold was selected so as not to overestimate alpha diversity, as intraspecific dissimilarity at this region of COI can reach 3–9% (Leray *et al.*, 2013). Representative sequences for each OTU were assigned taxonomy using the MIDORI “unique” database, and by LCA of GenBank *blastn* matches (Pedregosa *et al.*, 2011; Clark *et al.*, 2016; Machida *et al.*, 2017). All subsequent analyses were carried out in R 4.0.0 (R Development Core Team, 2009).

Statistical analyses

Statistical tests in R used “*phyloseq*,” “*vegan*,” and the *tidyverse* (Dixon, 2003; McMurdie and Holmes, 2013; Wickham *et al.*, 2019). Contaminant sequences were identified from negative controls with the combined method in “*decontam*,” with independent detection for each marker and sequencing run (Davis *et al.*, 2018). Contaminants were removed from all samples and negative controls were excluded from subsequent analyses. Sequences identified as non-metazoans, fishes, or mammals also were removed.

Samples were rarefied to 20,000 reads and 25,000 reads for 18S and COI, respectively, with samples falling below these thresholds removed. The relationship between rarefied observed richness, defined as OTU/ASV counts, and sequencing depth was tested with Spearman’s rank-order correlation. Appearance in PCR replicates was tested with a Kruskal-Wallis 1-way ANOVA, including only samples retaining at least three PCR replicates. Observed richness was plotted against the fraction of the plankton sample analyzed, illustrated with the nonparametric LOESS best fit.

To test whether relative read counts were correlated with independent ZooScan-based measures of biomass and abundance, zooplankton sequences were compared to numerical abundance and carbon biomass for taxonomic groups resolved using both digital imaging and at least one metabarcoding marker. Taxonomic groups were combined as necessary so that comparison groups were the same for both methods, including collapsing the fine taxonomic resolution that is present in metabarcoding data. Cnidarians and ctenophores were combined into a single category. Malacostracan sequences were compared against ZooScan-identified euphausiids and shrimp-like decapods. Comparisons were made for all thaliaceans together, and for salps, doliolids, and pyrosomes where identifiable. Separate comparisons were made for eucalanid copepods and for calanoid copepods excluding eucalanids. All data were converted to proportions and arcsine square root transformed, and

Pearson’s product-moment correlations were computed for each comparison, with Bonferroni correction.

Ethanol neutralization

To test the effects of ethanol neutralization with ammonium hydroxide on molecular diversity, three samples were collected near La Jolla Canyon using a 1 m diameter, 333 μm mesh ring-net surface tow on 18 December 2017 and near the CCE2 mooring (http://mooring.ucsd.edu/dev/cce2/cce2_12/) using a 0.71 m diameter, 202 μm mesh Bongo net towed obliquely to 180 m on 13–14 March 2018. Each sample was split quantitatively, and 50% preserved in unamended 95% non-denatured ethanol (pH 6.5) and 50% in 95% non-denatured ethanol neutralized with 5-mM ammonium hydroxide (final pH 8.0). These samples were analyzed using metabarcoding as described above, except were sequenced only at the COI marker. These samples were processed in their entirety, using multiple DNA extractions as necessary. Amplified samples were sequenced on two Illumina MiSeq runs, with each sample included in both runs (300bp paired-end V3). Sequences from replicate extractions and MiSeq runs were combined within each sample, and samples were rarefied to the lowest sequencing depth. Observed richness in the paired samples was compared using a Wilcoxon Matched Pairs Signed Rank test. Non-rarefied data were converted to relative abundances, samples clustered using average neighbor clustering based on Bray–Curtis distance and clusters tested for significance with a SIMPROF test. A PERMANOVA was subsequently used to test whether sampling event or preservation method affected observed community composition (Oksanen *et al.*, 2009).

Results

Bioinformatics

On average, 95% of reads demultiplexed by dual 8-mer indexing had the appropriate 6-mer indexes. A total of 12,923,747 sequences were recovered at the 18S marker, 6,882,057 of which passed quality and chimera filtering and were denoised into ASVs. After removal of 16 ASVs identified as contaminants and 280 non-metazoan, mammal, and fish ASVs, 966 ASVs were recovered at 18S. Of the 13,014,170 total COI sequences, 8,751,265 passed quality and chimera filtering. Removal of 19 contaminants and 105 non-metazoan, mammal, and fish OTUs resulted in 1943 OTUs at COI. Observed taxa spanned 17 phyla and included some meroplanktonic and parasitic species (Table 1). OTU rarefaction curves begin to reach saturation at 25,000 reads at COI, and 20,000 reads at 18S (Figure 1a and b). Despite rarefaction curves approaching saturation, richness was positively correlated with sequencing depth at COI (Figure 1c, $p = 2.7e-09$, $\rho = 0.411$, two-sided Spearman’s rank), and negatively correlated at 18S (Figure 1d, $p = 7.4e-12$, $\rho = -0.483$, two-sided Spearman’s rank). Analyses with non-rarefied data were similarly significant.

Sub-sampling and PCR replication

Each plankton subsample was analyzed with three independent PCR replicates with unique multiplexing indexes. There was no significant difference in community structure between PCR replicates, ($p \geq 0.05$, SIMPROF analysis of Bray-Curtis distance, not shown). However, there was some variability in the appearance of

Table 1. The number of OTUs or ASVs resolved by each marker for all taxa classified at least to phylum. OTU or ASV counts for each group are reported for both taxonomic assignment methods used and for both marker regions, such that a species can appear in each of the four columns independently. Taxa not classified to phylum are absent from this table.

| | COI OTUs | | 18S ASVs | |
|---------------------|----------|--------|----------|-------|
| | NCBI | MIDORI | NCBI | SILVA |
| Annelida | 47 | 18 | 54 | 49 |
| Arthropoda | 995 | 742 | 478 | 502 |
| Brachiopoda | – | – | 5 | 2 |
| Bryozoa | 12 | 8 | 1 | 1 |
| Chaetognatha | 19 | 5 | – | – |
| Chordata (Tunicata) | 9 | 1 | 53 | 50 |
| Cnidaria | 80 | 64 | 117 | 112 |
| Ctenophora | 4 | – | 9 | 6 |
| Echinodermata | 39 | 25 | 20 | 20 |
| Hemichordata | – | – | 2 | 2 |
| Mollusca | 142 | 30 | 38 | 35 |
| Nematoda | 2 | 1 | – | – |
| Nemertea | 6 | 2 | 3 | 3 |
| Phoronida | 1 | – | 2 | – |
| Platyhelminthes | 9 | 2 | 2 | 2 |
| Porifera | – | – | 3 | – |
| Sipuncula | 1 | – | 5 | 5 |

taxa between PCR replicates. Taxa that did not appear in all three PCR replicates tended to be lower rank order OTUs and ASVs that were less abundant based on sequence counts, but more abundant taxa were also often absent from one or more of the PCR replicates

(Figure 2, $p < 2.2e-16$, Kruskal–Wallis one-way ANOVA). Replicate analyses with non-rarefied data showed similar results.

Each zooplankton sample was subsampled to the maximum biomass possible for a single DNA extraction, resulting in different fractions of the parent sample being analyzed. Observed richness within subsamples increased with the fraction of parent sample analyzed, with richness appearing to saturate around 6.25%, or 1/16th of the initial bulk sample (Figure 3), for both markers. Richness was not correlated with the volume of seawater filtered (Figure 3, colour, Spearman's rank; COI: $p = 0.085$, $\rho = 0.124$; 18S: $p = 0.213$, $\rho = 0.094$). Replicate analyses with non-rarefied data found similar correlations and significance values.

Comparisons between imaging and sequencing

To test whether relative read abundance reflects community structure, read counts were compared with numerical abundance and carbon biomass from ZooScan analyses. Comparisons were made using proportions, as metabarcoding data are proportional (Lindque *et al.*, 2013; Hirai *et al.*, 2015), and were possible for 16 taxonomic groups of zooplankton, 12 of which were resolved at both metabarcoding markers. Of the 16 taxa analyzed, 15 groups showed a significant correlation ($P \leq 0.05$) between proportion of biomass and proportion of sequences at either COI, 18S, or both (Table 2), although the strength of the correlation was variable. More abundant taxa showed a stronger relationship between carbon biomass and sequences (Table 2, Figure 4). At COI, the strength of the relationship was significantly correlated with average proportion of sequences, but this relationship was not significant at 18S (Figure 4). There was some variability between markers, with oithonids, do-

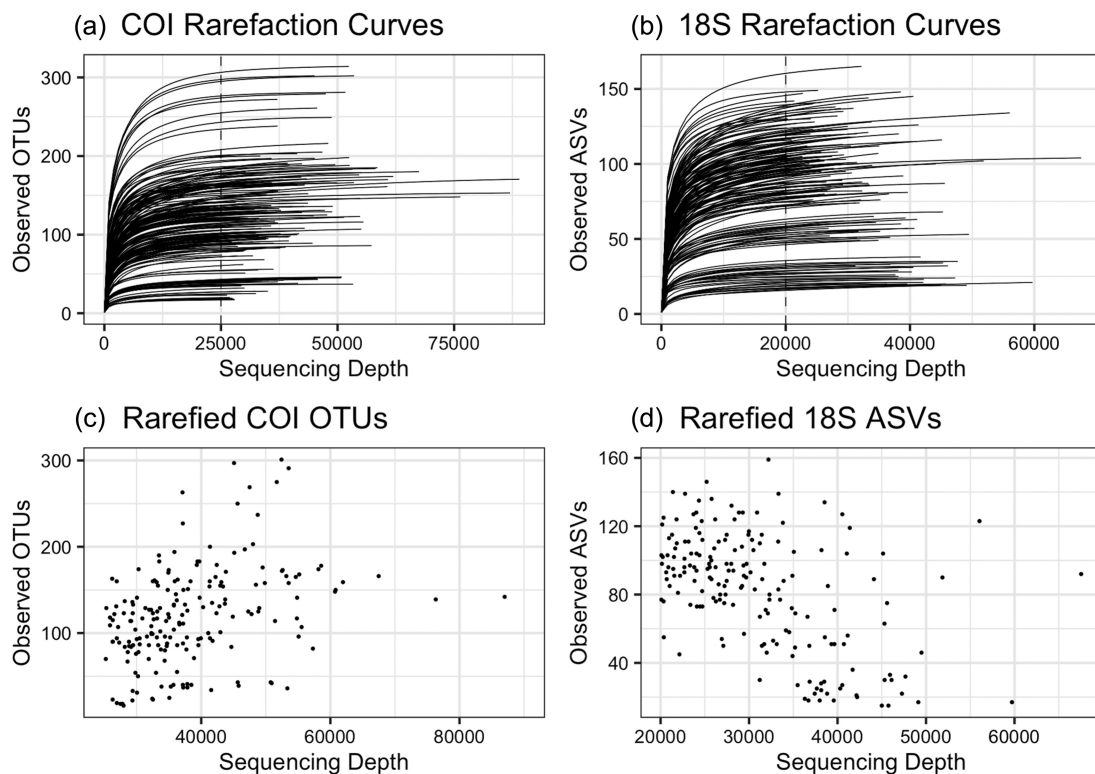


Figure 1. Rarefaction curves for (a) COI OTUs and (b) 18S ASVs, based on sequencing depth. Dashed lines represent the rarefaction depth for each marker. Richness, measured as observed OTUs/ASVs, increased with increasing sequencing depth at (c) COI, but not at (d) 18S.

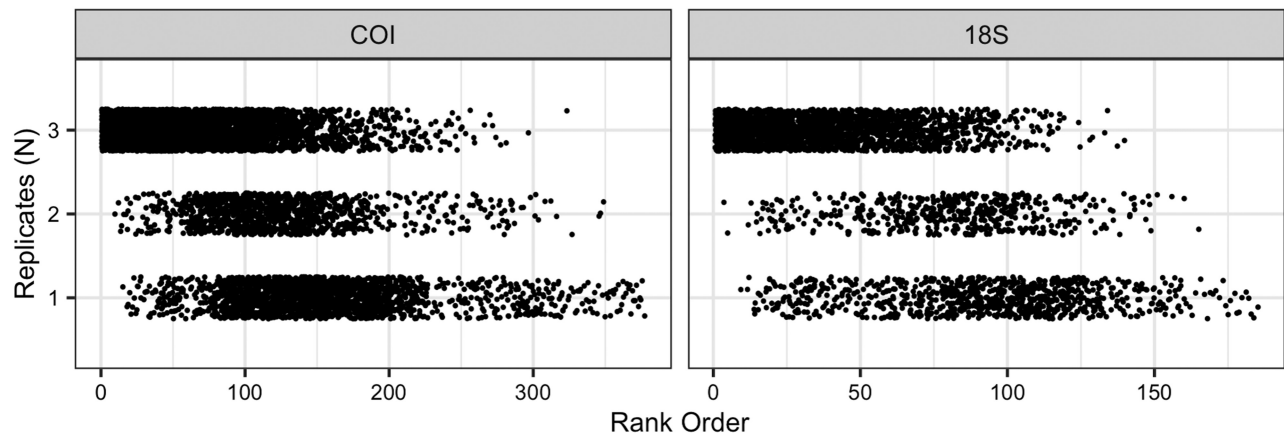


Figure 2. The number of PCR replicates in which each OTU/ASV occurs in relation to rank order of taxa. Rank order is based on summed abundance across PCR replicates. Higher rank order taxa (rarer) were less likely to occur in all three replicates, while low rank order taxa (dominants) tended to occur in more replicates. Data have been rarefied to 25000 and 20000 reads for COI and 18S, respectively.

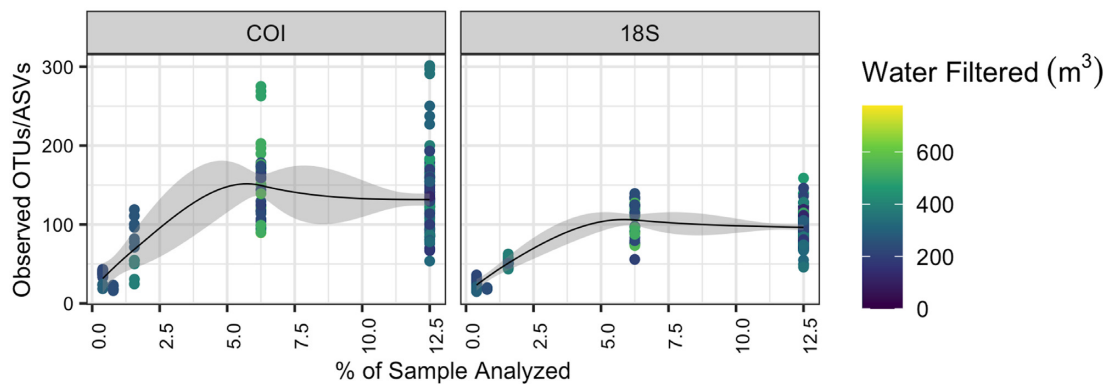


Figure 3. Observed richness at (left-hand panel) COI and (right-hand panel) 18S (in relation to the percentage of the zooplankton sample analyzed). For both markers, richness across all samples approached saturation at $\sim 6.25\%$ analyzed. Colour scale represents the total volume of seawater filtered at collection. Curves show the LOESS fit and shading represents 95% confidence intervals.

lioids, and pyrosomes only resolved at 18S and chaetognaths only resolved by COI. For most groups, the relationship between carbon biomass and sequence counts was equal to or stronger than the relationship between numerical abundance and sequence counts, with the exception of oithonids (Table 2, Figures S1 and S2). Chaetognath sequences did not show a significant relationship against either abundance or carbon biomass. Contrary to our expectation that crustaceans would show a better relationship than gelatinous organisms, there was not a close correspondence between tissue composition and strength of correlation between proportions of sequences and carbon biomass (Table 2).

A closer examination showed that there was wide scatter underlying even strong correlations. Figure 5 illustrates relationships for four representative taxa, showing two abundant copepod groups with stronger relationships and two other taxonomic groups (thaliaceans, ostracods) with weaker relationships and greater variability between markers, while Figures S1 and S2 include all taxa. Notably, there were some data points that were outliers in multiple correlations, such as those from Cycle 3, 250–400 m and Cycle 2, 200–250 and 350–400 m, which were found in the upper left quartile of the eucalanid correlation for both markers, and the lower right quartile for the calanoid correlation at COI (Figure 5). In addition to the taxa absent from one marker, there were taxa found at both markers that

showed stronger relationships at one. Ostracods showed a stronger relationship between COI reads and biomass, while thaliaceans had a strong relationship only at 18S (Figure 5).

Ethanol neutralization

For our test of ammonium hydroxide as a neutralizing agent, 494 COI OTUs were found. Total richness and richness within taxonomic groups were not significantly different between neutralized and untreated samples ($p = 0.22$, Wilcoxon, Figure 6) and there was no taxonomic bias, which would appear as a directional shift within points of a given color in Figure 5. Clustering of samples identified two significant groups separating by collection location (Figure S3, SIMPROF alpha = 0.05). A PERMANOVA revealed that preservation method had no effect on community structure, but that collection event was a significant predictor of observed community structure ($R^2 = 0.79$, $p = 0.002$). Parallel analyses with non-rarefied OTU tables and presence–absence data showed similar results.

Discussion

Our results provide a framework for interpreting metabarcoding results of zooplankton community composition. We found that tech-

Table 2. Pearson's correlation coefficient (R) and the significance level for all comparisons between proportion of sequences and proportion of biomass or numerical abundance (ZooScan-based measures). All proportions have been arcsine square root transformed.

| Taxon | Proportion carbon biomass vs. proportion sequences | | | | Proportion abundance vs. proportion sequences | | | | |
|-------------|--|-------|-------|------|---|-------|-------|-------|-----|
| | COI R | | 18S R | | COI R | | 18S R | | |
| Crustaceans | Eucalanids | 0.77 | *** | 0.72 | *** | 0.67 | *** | 0.66 | *** |
| | Calanoids | 0.81 | *** | 0.74 | *** | 0.72 | *** | 0.69 | *** |
| | Oithonids | – | – | 0.46 | *** | – | – | 0.64 | *** |
| | Poecilostomatoids | 0.37 | *** | 0.11 | *** | 0.11 | NS | –0.17 | NS |
| | Malacostracans | 0.58 | *** | 0.38 | *** | 0.64 | *** | 0.29 | *** |
| | Ostracods | 0.57 | *** | 0.19 | NS | 0.58 | *** | 0.36 | *** |
| Tunicates | Doliolids | – | – | 0.66 | *** | – | – | 0.65 | *** |
| | Pyrosomes | – | – | 0.9 | *** | – | – | 0.88 | *** |
| | Salps | 0.05 | NS | 0.09 | *** | 0.03 | NS | 0.09 | NS |
| | Thaliaceans | –0.03 | NS | 0.88 | *** | –0.01 | NS | 0.42 | *** |
| | Appendicularians | 0.22 | NS | 0.37 | *** | 0.19 | NS | 0.27 | NS |
| Other | Cnidarians & Ctenophores | 0.48 | *** | 0.36 | *** | 0.48 | *** | 0.18 | NS |
| | Bryozoans | 0.87 | *** | 0.72 | *** | 0.77 | *** | 0.62 | *** |
| | Polychaetes | 0.5 | *** | 0.58 | *** | 0.45 | *** | 0.55 | *** |
| | Pteropods | 0.39 | *** | 0.46 | *** | 0.62 | *** | 0.049 | *** |
| | Chaetognaths | –0.12 | NS | – | – | 0.03 | NS | – | – |

NS - not significant; * $p < 0.05$; ** $p < 0.01$; *** $p < 0.001$; Bonferroni corrected significance levels.

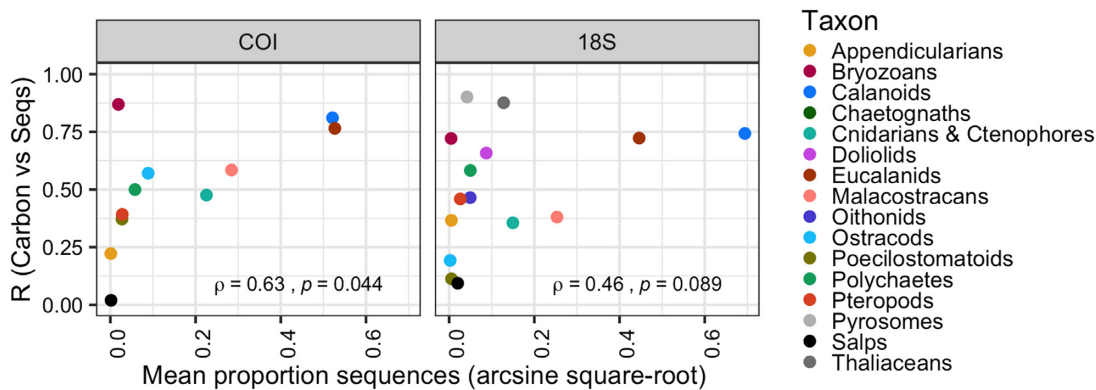


Figure 4. For each taxonomic group, Pearson's correlation coefficient (R) for the relationship between the proportion of sequences and proportion of carbon biomass is plotted against the average proportion of sequences across all samples. The strength of the correlation was stronger for more abundant groups at the COI marker, but the relationship at 18S was not significant ($p < 0.05$, Spearman's rank).

nical replication increases the detection of rare taxa and that sub-sampling has the potential to depress observed richness. In comparisons of relative read counts with morphological analyses, read abundance was positively correlated with the proportion of zooplankton biomass for all but one of the taxonomic groups analyzed, with considerable variability in the strength of the correlation among taxonomic groups. Thus, metabarcoding can be a viable approach for representing relative biomass of several major taxonomic groups but should be interpreted cautiously for less abundant taxa. In an important point for field fixation protocols, we found that neutralized ethanol provides unbiased measures of community composition.

Sub-sampling and PCR replication

We found a positive relationship between sequencing depth and richness at COI and a negative relationship at 18S. As sequencing depth is determined by sample pooling and library size (Herbold *et al.*, 2015), the observed relationships were primarily an artefact of library pooling. Parallel analyses with non-rarefied data were similar, indicating that the relationship was not an artefact of rarefaction (McMurdie and Holmes, 2014; Willis, 2019).

Good overall correspondence was observed between PCR replicates, although some taxa were absent from one or more PCR replicates. These taxa could be interpreted as spurious sequences arising from PCR errors, and some studies recommend removing OTUs

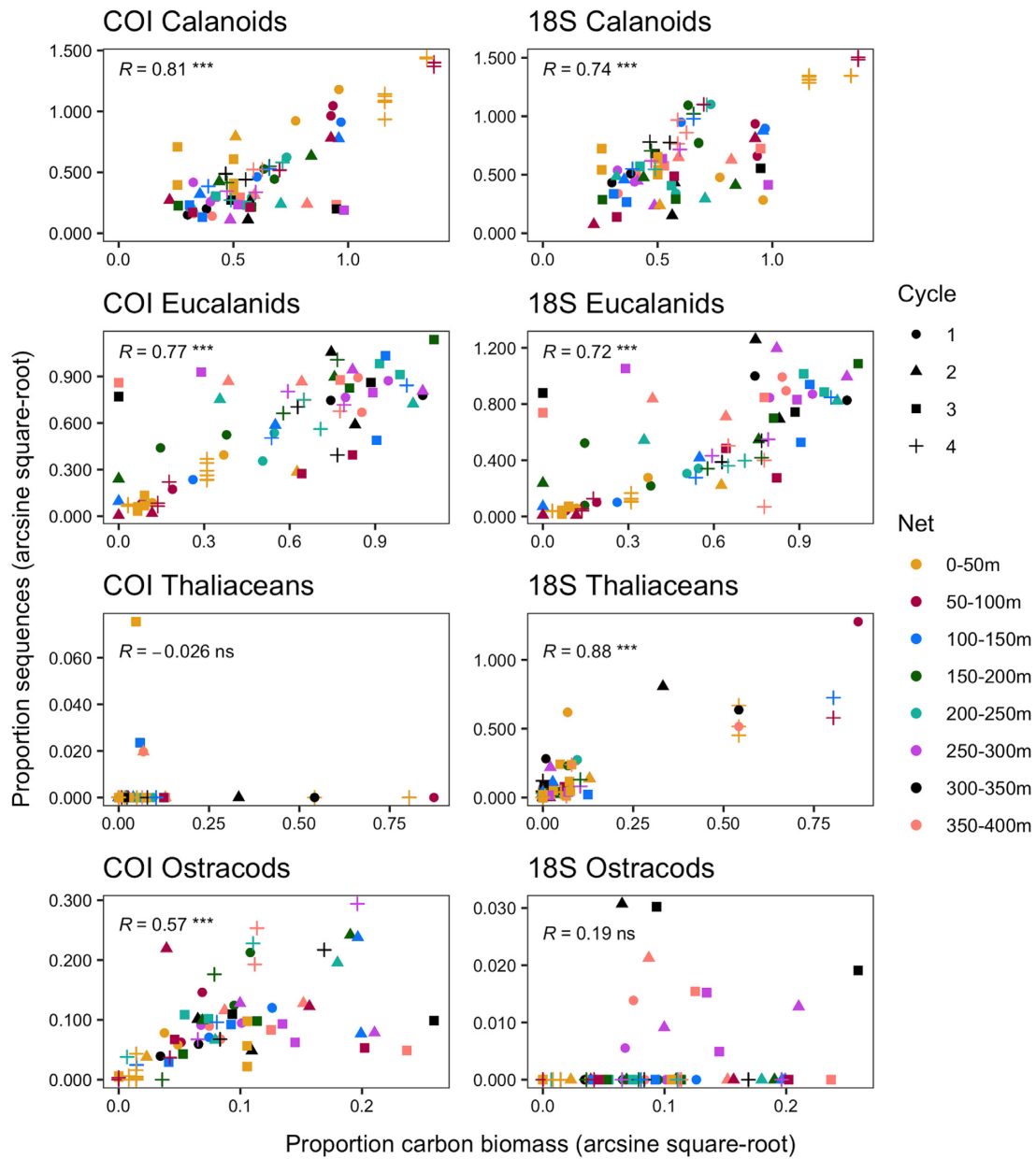


Figure 5. The proportion of metabarcoding sequences classified as calanoid, eucalanid, thaliacean, and ostracod in relation to the proportion of carbon biomass within the full zooplankton community, calculated from ZooScan ROIs. There is a strong positive relationship at both markers for the two copepod groups, and for thaliaceans at 18S and ostracods at COI. Note the different scales for each panel. All data have been arcsine square root transformed. Collection locations (Cycle, Net) are shown to enable comparison between taxa. Additional taxa and all abundance relationships are shown in Figures S1 and S2. (ns = $p > 0.05$, * $p < 0.05$, ** $p < 0.01$, *** $p < 0.001$).

that do not appear in all replicates (Loos and Nijland, 2020, but see also Lahoz-Monfort *et al.*, 2016). However, many of these taxa were found in higher abundance in nearby samples, indicating they represented rare individuals or fragments of animals. Multiple PCR replicates are widely recommended to minimize false negatives in environmental DNA studies (Ficetola *et al.*, 2016; Ruppert *et al.*, 2019). Stochastic variability in the detection of rare species has been observed in tissue-based metabarcoding analyses (Leray and Knowlton, 2017), and our results indicate that in a natural community this stochasticity can affect both rare and more abundant taxa. For our study site, at least three PCR replicates were necessary to

fully capture the diversity of the zooplankton community, and we recommend this for other regions as well.

Richness increased as a function of the fraction of the sample analyzed and appeared to saturate at around 6.25% of the sample. This comparison was made across ocean environments from nearshore upwelling dominated by a few taxa to higher diversity, offshore mesotrophic waters, and at depths ranging from the surface to 400 m. Addition of replicate subsamples resulted in species accumulation curves closely matching that of the full sample set, indicating that the low richness is an artefact of subsampling. Our results indicate that in addition to technical replication, a minimum

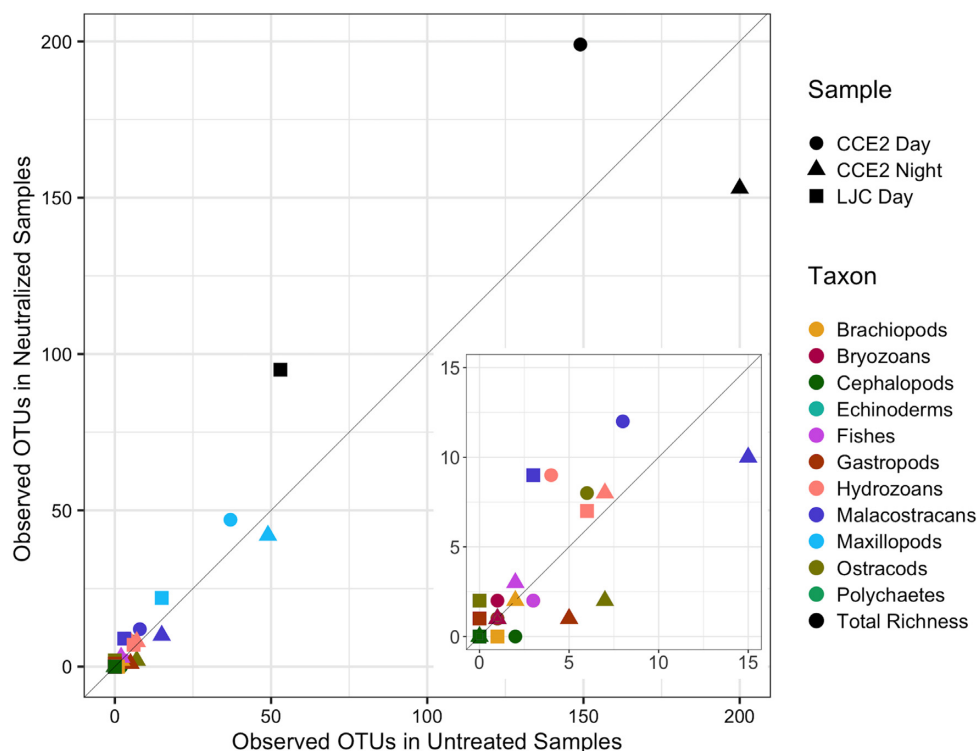


Figure 6. Comparison of number of COI OTUs from paired samples preserved in ethanol neutralized with ammonium hydroxide with those in unamended ethanol. The diagonal is the 1:1 line. Colours indicate zooplankton taxa; symbols indicate the three sets of samples compared. Inset shows OTUs at low counts. There was no difference in overall richness and no taxonomic bias between neutralized and untreated samples.

fraction of the initial bulk sample should be analyzed. For zooplankton assemblages in our region, this threshold was $> 6.25\%$ of the sample, but this value should be estimated for other ocean ecosystems with distinct rank abundance profiles.

The importance of replicate field samples, subsampling, PCR replication, and sequencing depth are likely to vary between ecosystems and study designs, with greater replication at all stages necessary for more diverse systems and increased field sampling effort in systems with high spatial variability. Metabarcoding analyses should be designed with careful consideration of the goals of the study and the types of variability present in the ecosystem of interest (Kelly *et al.*, 2019).

Comparisons between imaging and sequencing

The relationships between carbon biomass and read abundance were stronger for more abundant groups. We found strong relationships at one or both markers for eucalanid and calanoid copepods, malacostracans, ostracods, bryozoans, and polychaetes. Several previous analyses have reported positive relationships between read counts and abundance or biomass within the zooplankton community, for a range of taxonomic groups and marker regions (Harvey *et al.*, 2017; Bucklin *et al.*, 2019; Schroeder *et al.*, 2020). The strong positive relationships we observed for more abundant taxa corroborate these studies, and we similarly found that such relationships are not always significant.

The poor or non-significant relationships observed for some groups are also important, as they help inform the limitations of estimating biomass or abundance from read counts. Because metabarcoding data are proportional, biases introduced by variability in gene copy number, amplification efficiency or primer

bias propagate to all taxa within a sample (McLaren *et al.*, 2019). In our analysis, some of these biases can be seen in the absence of oithonid copepods, doliolids, and salps at COI, of chaetognaths at 18S, and in the better relationships for ostracods and thaliaceans at COI and 18S, respectively. Approaches to account for bias in amplicon data sets, including the use of taxon: taxon proportions or estimation of amplification efficiency from known community composition, often require mock communities or independent data on community composition or primer bias which are less available for zooplankton than for microbial communities (Kelly *et al.*, 2019; McLaren *et al.*, 2019). Our analyses indicate that these normalization procedures could be particularly important for less abundant taxonomic groups.

There was a notable difference between the strengths of relationships observed at different taxonomic levels within a group. For thaliaceans as a whole, there was a strong correlation between proportion biomass and proportion sequences at 18S. However, this relationship was due to good correspondence for doliolids and pyrosomes, while that for salps was quite low. Chaetognath COI sequences and biomass or abundance were not correlated, but chaetognath sequences were only recovered from mesopelagic species while chaetognaths were identifiable from ZooScan images throughout the water column. Similarly, ostracods at 18S were only detected in mesopelagic samples, while ostracods were found in all samples using COI or using ZooScan imaging. These mismatches may be due to poor representation in the NCBI, MIDORI, and SILVA databases used to assign taxonomy, or due to variability in amplification efficiency between species present in different depth zones. Previous work has found that agreement between methods increases as species are grouped at coarser taxonomic levels (Leray and Knowlton, 2015; Harvey *et al.*, 2017). In contrast, our

data indicate that relationships can be either strengthened or weakened at coarser taxonomic resolution, depending on the variance in marker performance between closely related taxa. We recommend that marker biases be accounted for and that estimates of relative abundance and comparisons between survey methods be limited to taxa that are well resolved.

Some outlying samples were clearly visible in the scatterplots of eucalanid and calanoid relationships (Figure 5). These samples were outliers for both marker regions, and incorrect classification with independent reference databases is unlikely. Further verifications of image classifications did not detect misidentifications. It is most likely that these samples reflect a true mismatch in the detection capabilities of the molecular and imaging methods compared. The outliers in question were collected from the upper mesopelagic (200–400 m) and likely included eucalanid copepodites that were not easily identifiable to genus by digital imaging (hence only assigned to calanoid copepods) but were classifiable as eucalanids by metabarcoding. Digital imaging lacks the morphological detail necessary to identify most species, especially for young developmental stages, hence comparisons must be made at more aggregated taxonomic levels. However, ZooScanning accurately reflects body sizes (Gorsky *et al.*, 2010) and numerical abundances (Whitmore *et al.*, 2019) when compared to other methods. Conversions from body length to carbon biomass introduce another source of uncertainty, but were optimized for the zooplankton taxa of our study region (Lavaniegos and Ohman, 2007) and are unlikely to bias the biomass proportions calculated here. These outlier samples illustrate the strengths of combining multiple observation methods. While metabarcoding lacks information such as body size, sex, or life history stage, it can increase detection sensitivity to rarer species or taxa that are undetected by visual surveys or other collection methods (Stat *et al.*, 2019). Because metabarcoding does not yield measurements of absolute abundance, we recommend that metabarcoding and morphological or imaging methods be used in combination.

Ethanol neutralization

For our comparison of paired samples preserved in either unamended ethanol or ethanol neutralized with ammonium hydroxide, we recovered fewer OTUs than were found in the full data set, likely due to limited sampling. However, the observed OTUs included a similar taxonomic range. We did not detect any effect of ammonium hydroxide on community structure, composition, or richness between the two sets of samples. These results indicate that ammonium hydroxide addition to ethanol (Bednaršek and Ohman, 2015) permits a single fixative to be used for both molecular and morphological analyses, including calcareous zooplankton. This result bears confirmation with other DNA extraction protocols.

Supplementary data

Supplementary material is available at the ICESJMS online version of the manuscript.

Data availability

OTU tables, fasta files, and sample metadata are available through CCE-LTER DataZoo. Raw sequence are under NCBI SRA PRJNA679794. Code is available at < https://github.com/sammatthews/Matthews_et_al_IJMS_2021 >

Acknowledgements

Thanks to the California Current Ecosystem LTER program, the R/V Sikuliaq, and P. Zerofski for sample collections. E. Tovar and H. Zheng assisted with laboratory work. The SIO Pelagic Invertebrate Collection provided access to zooplankton samples. We thank L. Hauser and two anonymous reviewers for constructive comments on this manuscript. Support was provided by a US NSF Graduate Research Fellowship to S. Matthews, NSF to the California Current Ecosystem LTER site, and by Gordon and Betty Moore Foundation support to MDO. This study is a contribution to the Scientific Committee on Oceanic Research (SCOR) working group 157 (MetaZooGene).

References

- Bednaršek, N., Klinger, T., Harvey, C. J., Weisberg, S., McCabe, R. M., Feely, R. A., Newton, J. *et al.* 2017. New ocean, new needs: application of pteropod shell dissolution as a biological indicator for marine resource management. *Ecological Indicators*, 76: 240–244.
- Bednaršek, N., and Ohman, M. D. 2015. Changes in pteropod distributions and shell dissolution across a frontal system in the California Current System. *Marine Ecology Progress Series*, 523: 93–103.
- Bolyen, E., Rideout, J. R., Dillon, M. R., Bokulich, N. A., Abnet, C., Al-Ghalith, G. A., Alexander, H. *et al.* 2018. QIIME 2: reproducible, interactive, scalable, and extensible microbiome data science. *Peer J Inc*, 1: e27295v2.
- Braukmann, T. W. A., Ivanova, N. V., Prosser, S. W. J., Elbrecht, V., Steinke, D., Ratnasingham, S., de Waard, J. R. *et al.* 2019. Metabarcoding a diverse arthropod mock community. *Molecular Ecology Resources*, 19: 711–727.
- Brisbin, M. M., Brunner, O. D., Grossmann, M. M., and Mitarai, S. 2020. Paired high-throughput, *in situ* imaging and high-throughput sequencing illuminate acantharian abundance and vertical distribution. *Limnology and Oceanography*. 65 : 2954–2965 .
- Brown, E. A., Chain, F. J. J., Crease, T. J., MacIsaac, H. J., and Cristescu, M. E. 2015. Divergence thresholds and divergent biodiversity estimates: can metabarcoding reliably describe zooplankton communities? *Ecology and Evolution*, 5: 2234–2251.
- Bucklin, A., Yeh, H. D., Questel, J. M., Richardson, D. E., Reese, B., Copley, N. J., and Wiebe, P. H. 2019. Time-series metabarcoding analysis of zooplankton diversity of the NW Atlantic continental shelf. *ICES Journal of Marine Science*, 76: 1162–1176.
- Callahan, B. J., McMurdie, P. J., Rosen, M. J., Han, A. W., Johnson, A. J. A., and Holmes, S. P. 2016. DADA2: high-resolution sample inference from Illumina amplicon data. *Nature Methods*, 13: 581–583.
- Clark, K., Karsch-Mizrachi, I., Lipman, D. J., Ostell, J., and Sayers, E. W. 2016. *Nucleic Acids Research*, 44: D67–D72.
- Clarke, L. J., Beard, J. M., Swadling, K. M., and Deagle, B. E. 2017. Effect of marker choice and thermal cycling protocol on zooplankton DNA metabarcoding studies. *Ecology and Evolution*, 7: 873–883.
- Costello, M., Fleharty, M., Abreu, J., Farjoun, Y., Ferriera, S., Holmes, L., Granger, B. *et al.* 2018. Characterization and remediation of sample index swaps by non-redundant dual indexing on massively parallel sequencing platforms. *Bmc Genomics [Electronic Resource]*, 19: 332.
- Davis, N. M., Proctor, D. M., Holmes, S. P., Relman, D. A., and Callahan, B. J. 2018. Simple statistical identification and removal of contaminant sequences in marker-gene and metagenomics data. *Microbiome*, 6: 226. .
- Dixon, P. 2003. VEGAN, a package of R functions for community ecology. *Journal of Vegetation Science*, 14: 927–930.
- Elbrecht, V., and Leese, F. 2015. Can DNA-based ecosystem assessments quantify species abundance? Testing primer bias and Biomass—Sequence relationships with an innovative metabarcoding protocol M. Hajibabaei [ed.]. *Plos One*, 10: e0130324.
- Ellen, J., Li, H., and Ohman, M. 2015. Quantifying California current plankton samples with efficient machine learning techniques. OCEANS 2015 – MTSIEEE Washington. Institute of Electrical and Electronics Engineers Inc: Washington, United States .

- Ficetola, G. F., Taberlet, P., and Coissac, E. 2016. How to limit false positives in environmental DNA and metabarcoding? *Molecular Ecology Resources*, 16: 604–607.
- Frolander, H. F. 1968. Statistical variation in zooplankton numbers from subsampling with a stempel pipette. *Water Pollution Control Federation*, 40: R82–R88.
- Gorsky, G., Ohman, M. D., Picheral, M., Gasparini, S., Stemmann, L., Romagnan, J. - B., Cawood, A. *et al.* 2010. Digital zooplankton image analysis using the ZooScan integrated system. *Journal of Plankton Research*, 32: 285–303.
- Harvey, J. B. J., Johnson, S. B., Fisher, J. L., Peterson, W. T., and Vri-jenhoek, R. C. 2017. Comparison of morphological and next generation DNA sequencing methods for assessing zooplankton assemblages. *Journal of Experimental Marine Biology and Ecology*, 487: 113–126.
- Herbold, C. W., Pelikan, C., Kuzyk, O., Hausmann, B., Angel, R., Berry, D., and Loy, A. 2015. A flexible and economical barcoding approach for highly multiplexed amplicon sequencing of diverse target genes. *Frontiers in Microbiology*, 6: p731.
- Hirai, J., Kuriyama, M., Ichikawa, T., Hidaka, K., and Tsuda, A. 2015. A metagenetic approach for revealing community structure of marine planktonic copepods. *Molecular Ecology Resources*, 15: 68–80.
- Hirai, J., Nagai, S., and Hidaka, K. 2017. Evaluation of metagenetic community analysis of planktonic copepods using Illumina MiSeq: comparisons with morphological classification and metagenetic analysis using Roche 454. *Plos One*, 12: e0181452.
- Kelly, R. P., Shelton, A. O., and Gallego, R. 2019. Understanding PCR processes to draw meaningful conclusions from environmental DNA studies. *Scientific Reports*, 9: 12133.
- Laakmann, S., Blanco-Bercial, L., and Cornils, A. 2020. The crossover from microscopy to genes in marine diversity: from species to assemblages in marine pelagic copepods. *Philosophical Transactions of the Royal Society B: Biological Sciences*, 375: 20190446.
- Lahoz-Monfort, J. J., Guillera-Arroita, G., and Tingley, R. 2016. Statistical approaches to account for false-positive errors in environmental DNA samples. *Molecular Ecology Resources*, 16: 673–685.
- Lavaniegos, B. E., and Ohman, M. D. 2007. Coherence of long-term variations of zooplankton in two sectors of the California Current System. *Progress in Oceanography*, 75: 42–69.
- Leray, M., and Knowlton, N. 2015. DNA barcoding and metabarcoding of standardized samples reveal patterns of marine benthic diversity. *Proceedings of the National Academy of Sciences*, 112: 2076–2081.
- Leray, M., and Knowlton, N. 2017. Random sampling causes the low reproducibility of rare eukaryotic OTUs in Illumina COI metabarcoding. *Peer J*, 5: e3006.
- Leray, M., Yang, J. Y., Meyer, C. P., Mills, S. C., Agudelo, N., Ranwez, V., Boehm, J. T. *et al.* 2013. A new versatile primer set targeting a short fragment of the mitochondrial COI region for metabarcoding metazoan diversity: application for characterizing coral reef fish gut contents. *Frontiers in Zoology*, 10: 34.
- Lindeque, P. K., Parry, H. E., Harmer, R. A., Somerfield, P. J., and Atkinson, A. 2013. Next generation sequencing reveals the hidden diversity of zooplankton assemblages. *Plos One*, 8: e81327.
- Machida, R. J., Leray, M., Ho, S. - L., and Knowlton, N. 2017. Metazoan mitochondrial gene sequence reference datasets for taxonomic assignment of environmental samples. *Scientific Data*, 4: 170027.
- Martin, M. 2011. Cutadapt removes adapter sequences from high-throughput sequencing reads. *EMBnet journal*, 17: 10–12.
- McLaren, M. R., Willis, A. D., and Callahan, B. J. 2019. Consistent and correctable bias in metagenomic sequencing experiments. *eLife*, 8: e46923.
- McMurdie, P. J., and Holmes, S. 2013. phyloseq: an R package for reproducible interactive analysis and graphics of microbiome census data. *Plos One*, 8: e61217.
- McMurdie, P. J., and Holmes, S. 2014. Waste Not, Want Not: why rarefying microbiome data is inadmissible. *PLoS Computational Biology*, 10: e1003531.
- Oakes, R. L., Peck, V. L., Manno, C., and Bralower, T. J. 2019. Impact of preservation techniques on pteropod shell condition. *Polar Biology*, 42: 257–269.
- Ohman, M. D., Powell, J. R., Picheral, M., and Jensen, D. W. 2012. Mesozooplankton and particulate matter responses to a deep-water frontal system in the southern California Current System. *Journal of Plankton Research*, 34: 815–827.
- Ohman, M., Barbeau, K., Franks, P., Goericke, R., Landry, M., and Miller, A. 2013. Ecological transitions in a coastal upwelling ecosystem. *Oceanography*, 26: 210–219.
- Oksanen, J., Blanchet, F. G., Kindt, R., Legendre, P., Minchin, P. R., O'hara, R. B., Simpson, G. L., *et al.* 2009. The vegan Package.
- Pedregosa, F., Varoquaux, G., Gramfort, A., Michel, V., Thirion, B., Grisel, O., Blondel, M., *et al.*, 2011. Scikit-learn: machine Learning in Python. *Mach Learn Python*, 6: pp. 2825–2830.
- R Development Core Team. 2009. R: A Language and Environment for Statistical Computing, R Foundation for Statistical Computing. <https://www.r-project.org/> (last accessed 24 April 2020).
- Rognes, T., Flouri, T., Nichols, B., Quince, C., and Mahé, F. 2016. VSEARCH: a versatile open source tool for metagenomics. *Peer J*, 4: e2584.
- Ruppert, K. M., Kline, R. J., and Rahman, M. S. 2019. Past, present, and future perspectives of environmental DNA (eDNA) metabarcoding: a systematic review in methods, monitoring, and applications of global eDNA. *Global Ecology and Conservation*, 17: e00547.
- Santoferrara, L. F. 2019. Current practice in plankton metabarcoding: optimization and error management. *Journal of Plankton Research*, 41: 571–582.
- Schroeder, A., Stanković, D., Pallavicini, A., Gionchetti, F., Pansera, M., and Camatti, E. 2020. DNA metabarcoding and morphological analysis—assessment of zooplankton biodiversity in transitional waters. *Marine Environmental Research*, 160: 104946.
- Sommer, S. A., Woudenberg, L. V., Lenz, P. H., Cepeda, G., and Goetze, E. 2017. Vertical gradients in species richness and community composition across the twilight zone in the North Pacific Subtropical Gyre. *Molecular Ecology*, 26: 6136–6156.
- Stat, M., John, J., DiBattista, J. D., Newman, S. J., Bunce, M., and Harvey, E. S. 2019. Combined use of eDNA metabarcoding and video surveillance for the assessment of fish biodiversity. *Conservation Biology*, 33: 196–205.
- van der Loos, L. M., and Nijland, R. 2020. Biases in bulk: DNA metabarcoding of marine communities and the methodology involved. *Molecular Ecology*.
- van Guelpen, L., Markle, D. F., and Duggan, D. J. 1982. An evaluation of accuracy, precision, and speed of several zooplankton subsampling techniques. *ICES Journal of Marine Science*, 40: 226–236.
- Whitmore, B. M., Nickels, C. F., and Ohman, M. D. 2019. A comparison between Zooglider and shipboard net and acoustic mesozooplankton sensing systems. *Journal of Plankton Research*, 41: 521–533.
- Wickham, H., Averick, M., Bryan, J., Chang, W., D'Agostino McGowan, L., François, R., Grolemund, G. *et al.* 2019. Welcome to the Tidyverse. *Journal of Open Source Software*, 4: 1686.
- Willis, A. D. 2019. Rarefaction, Alpha Diversity, and Statistics. *Frontiers in Microbiology*, 10: p. 2407.
- Yilmaz, P., Parfrey, L. W., Yarza, P., Gerken, J., Pruesse, E., Quast, C., Schweer, T. *et al.* 2014. The SILVA and “All-species Living Tree Project (LTP)” taxonomic frameworks. *Nucleic Acids Research*, 42: D643–D648.
- Zhan, A., Hulák, M., Sylvester, F., Huang, X., Adebayo, A. A., Abbott, C. L., Adamowicz, S. J. *et al.* 2013. High sensitivity of 454 pyrosequencing for detection of rare species in aquatic communities. *Methods in Ecology and Evolution*, 4: 558–565.

Handling editor: Lorenz Hauser

All Taxa: Proportion Read Counts vs. Proportion Biomass

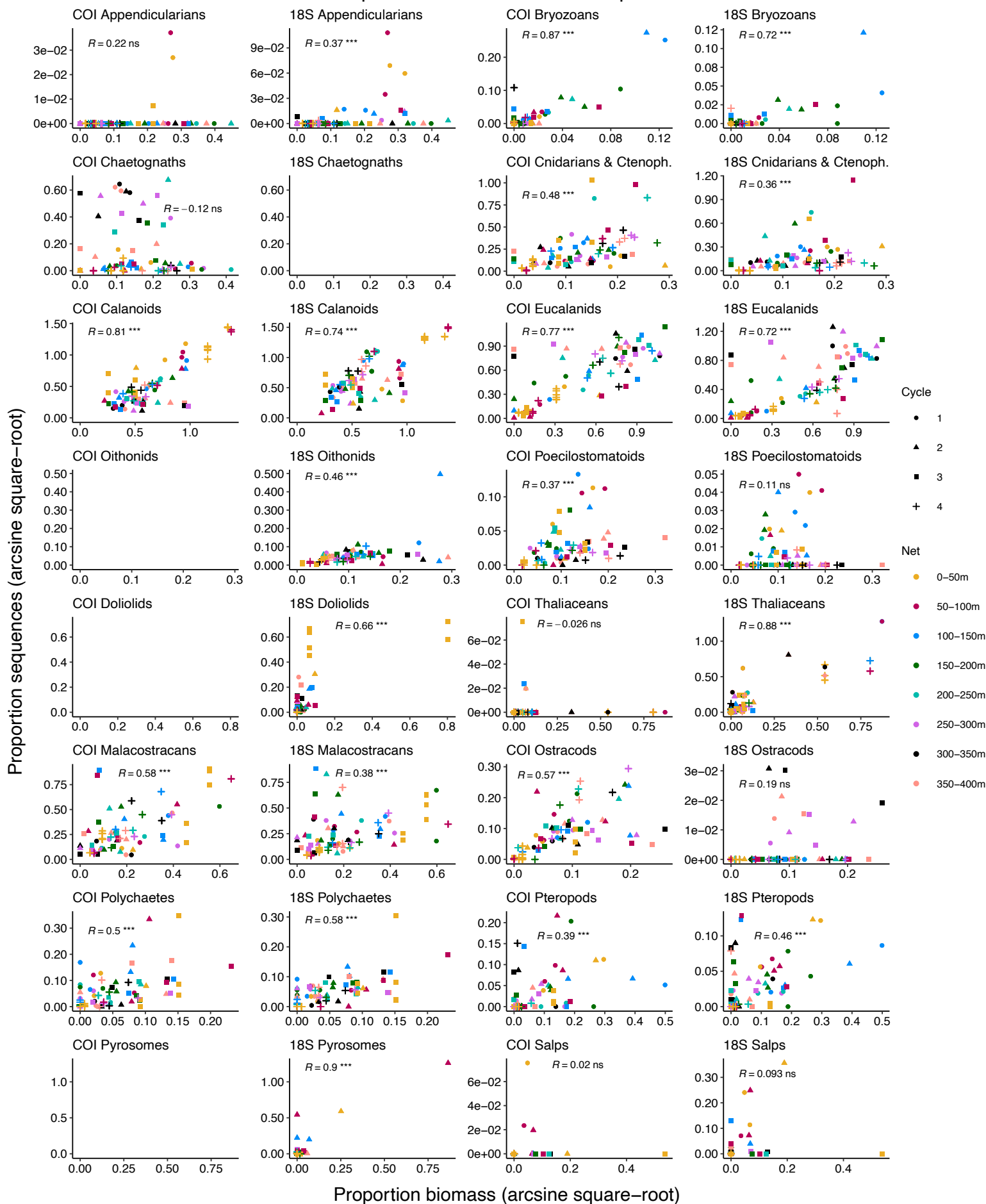


Figure S1. The proportion of metabarcoding sequences for each taxonomic group is plotted against the proportion of carbon biomass of the group within the full zooplankton community, calculated from Zooscan ROIs. Collection location (Cycle, Net) is shown to enable comparison between taxa. Blank panels are due to the absence of data at that marker. Note the different scales for each panel. (ns = $p > 0.05$, * $p < 0.05$, ** $p < 0.01$, *** $p < 0.001$).

All Taxa: Proportion Read Counts vs. Proportion Abundance

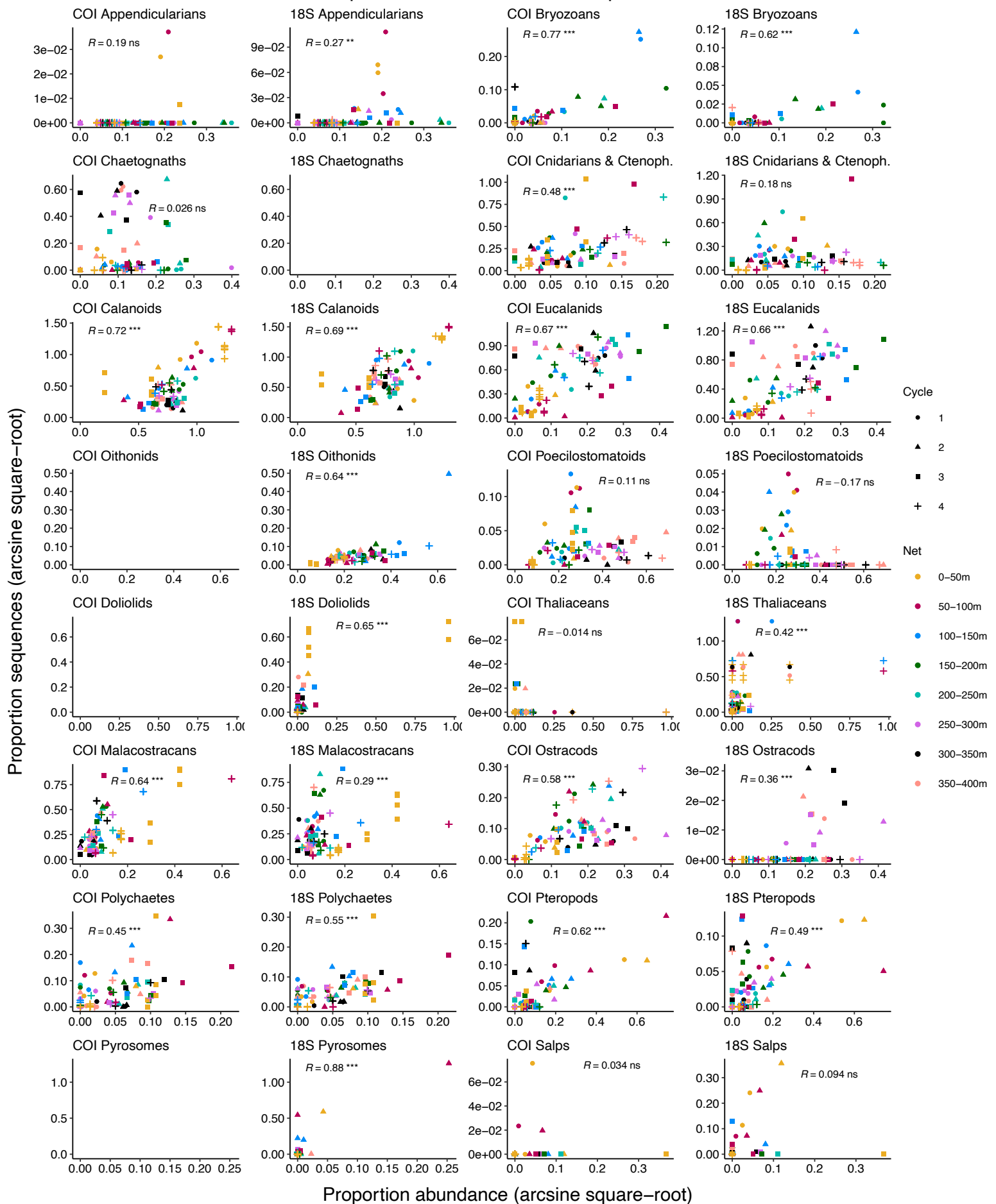


Figure S2. The proportion of metabarcoding sequences for each taxonomic group is plotted against the proportion of numerical abundance of the group within the full zooplankton community, calculated from Zooscan ROIs. Collection location (Cycle, Net) is shown to enable comparison between taxa. Blank panels are due to the absence of data at that marker. Note the different scales for each panel. (ns = $p > 0.05$, * $p < 0.05$, ** $p < 0.01$, *** $p < 0.001$).

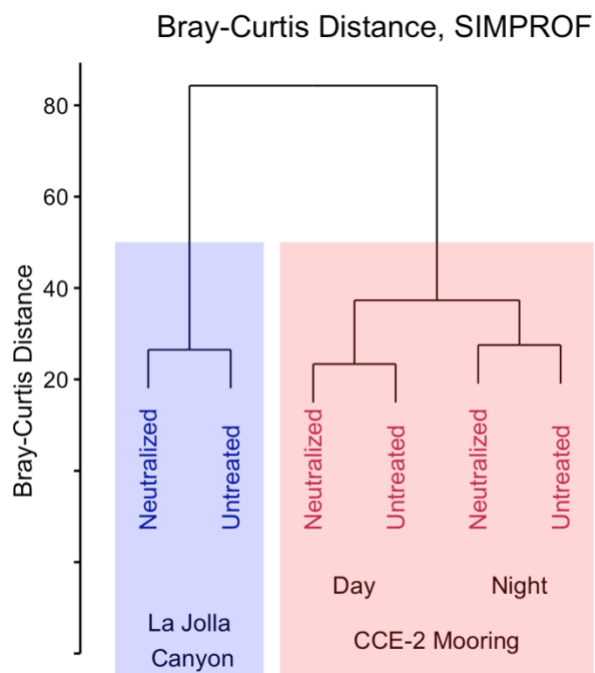


Figure S3. A SIMPROF test with average-neighbor clustering based on Bray Curtis distances. Clusters with non-significant structure are highlighted in blue and red boxes, respectively. Samples collected from two different locations were significantly different, but there was no difference between paired samples preserved in either neutralized or untreated ethanol.

Table S2. Primer sequences and PCR protocols for both PCR steps for 18S and COI. Red Xs represent variable indexing region, with per-sample indexes found in Table S1.

| 18S PCR 1 | | | |
|------------------|-----------------|---|--|
| Primers | Primer name | Primer Sequence | |
| | | Uni18S | TCGTCGGCAGCGTCAGATGTGTATAAGAGACAGXXXXXXXXAGGGCAAKYCTGGTGCCAGC |
| | Uni18SR | GTCTCGTGGGCTCGGAGATGTGTATAAGAGACAGXXXXXXXXGRCGGTATCTRATCGYCTT | |
| Reaction Volumes | Reagent | Volume | |
| | MiFi mix | 10 µl | |
| | BSA | 0.4 µl | |
| | dH2O | 6.6 µl | |
| | DNA template | 1 µl | |
| | Primer 1 | 1 µl | |
| | Primer 2 | 1 µl | |
| PCR Cycling | Temperature (°) | Time (MM:SS) | Cycles |
| | 95 | 3:00 | |
| | 95 | 0:15 | 28x |
| | 52 | 0:30 | |
| | 72 | 0:15 | |
| 72 | 5:00 | | |
| 18S PCR 2 | | | |
| Primers | Primer name | Primer Sequence | |
| | | Tag_F | AATGATACGGGACACCAGATCTACACXXXXXXXXTCGTCGGCAGCGTCAGATGTG |
| | Tag_R | CAAGCAGAAGACGGCATAACGAGATXXXXXXXXGTCTCGTGGGCTCGGAGATGTGTA | |
| Reaction Volumes | Reagent | Volume | |
| | MiFi mix | 7.5 µl | |
| | BSA | 0.3 µl | |
| | dH2O | 4.2 µl | |
| | DNA template | 1 µl | |
| | Primer 1 | 1 µl | |
| | Primer 2 | 1 µl | |
| PCR Cycling | Temperature (°) | Time (MM:SS) | Cycles |
| | 95 | 3:00 | |
| | 95 | 0:30 | 10x |
| | 55 | 0:30 | |
| | 72 | 0:45 | |
| 72 | 5:00 | | |
| COI PCR 1 | | | |
| Primers | Primer name | Primer Sequence | |
| | | cgLCO1490 | TCGTCGGCAGCGTCAGATGTGTATAAGAGACAGXXXXXXXXGGWACWGGWTGAACWGTWTAAYCCYCC |
| | cgHCO2198 | GTCTCGTGGGCTCGGAGATGTGTATAAGAGACAGXXXXXXXXTAIACYTCIGGRTGICRAARAAYCA | |
| Reaction Volumes | Reagent | Volume | |
| | MiFi mix | 10 µl | |
| | BSA | 0.4 µl | |
| | dH2O | 6.6 µl | |
| | DNA template | 1 µl | |
| | Primer 1 | 1 µl | |
| | Primer 2 | 1 µl | |
| PCR Cycling | Temperature (°) | Time (MM:SS) | Cycles |
| | 95 | 3:00 | |
| | 95 | 0:15 | 28x |
| | 48 | 0:30 | |
| | 72 | 0:15 | |
| 72 | 5:00 | | |
| COI PCR2 | | | |
| Primers | Primer name | Primer Sequence | |
| | | Tag_F | AATGATACGGGACACCAGATCTACACXXXXXXXXTCGTCGGCAGCGTCAGATGTG |
| | Tag_R | CAAGCAGAAGACGGCATAACGAGATXXXXXXXXGTCTCGTGGGCTCGGAGATGTGTA | |
| Reaction Volumes | Reagent | Volume | |
| | MiFi mix | 7.5 µl | |
| | BSA | 0.3 µl | |
| | dH2O | 4.2 µl | |
| | DNA template | 1 µl | |
| | Primer 1 | 1 µl | |
| | Primer 2 | 1 µl | |
| PCR Cycling | Temperature (°) | Time (MM:SS) | Cycles |
| | 95 | 3:00 | |
| | 95 | 0:30 | 10x |
| | 55 | 0:30 | |
| | 72 | 0:45 | |
| 72 | 5:00 | | |